Electronic structure of decagonal $Al_{65}Co_{15}Cu_{20}$ and $Al_{70}Co_{15}Ni_{15}$

Z.M. Stadnik* and G.W. Zhang
Department of Physics, University of Ottawa, Ottawa, Ontario, Canada K1N 6N5

A.-P. Tsai and A. Inoue
Institute for Materials Research, Tohoku University, Sendai 980, Japan
(Received 21 December 1994)

Photoemission spectroscopy measurements in the photon-energy range 35–120 eV have been used to make determinations of the valence bands of high-quality decagonal alloys $Al_{65}Co_{15}Cu_{20}$ and $Al_{70}Co_{15}Ni_{15}$. Resonance photoemission near the Co $3p \rightarrow 3d$ transition has been employed to show that the feature in the valence bands of both alloys with a maximum intensity at 0.7(2) eV below the Fermi level is predominantly of the Co $3p$ character. The feature at 3.7(1) eV in the valence band of $Al_{65}Co_{15}Cu_{20}$ has been identified as being mainly of the Cu $3d$ character, whereas the feature due to the Ni $3d$ states overlaps with the Co $3d$-like feature in the valence band of $Al_{70}Co_{15}Ni_{15}$. Within the energy resolution, our results reveal that, contrary to the prediction of recent band-structure calculations and to the widespread qualitative interpretation of various electronic transport data, there is no pseudogap in the density of states at the Fermi level in both decagonal alloys. This shows that decagonal alloys differ significantly in their electronic structure from icosahedral alloys and that a Hume-Rothery mechanism cannot be invoked to explain their stability and electronic transport properties. The need of high-energy-resolution photoemission experiments, which were shown to be essential to observe the theoretically predicted fine structure in the density of states, has been emphasized. The possible influence of chemical and topological disorder on the electronic structure of high-quality stable quasicrystals was indicated. A review of published experimental data on the electronic structure of decagonal alloys has also been presented.

I. INTRODUCTION

Quasicrystals (QC's) are a new form of matter which differs from the other two known forms, crystalline and amorphous, by possessing a new type of long-range translational order, quasiperiodicity, and a noncrystallographic orientational order associated with the classically forbidden fivefold (icosahedral), eightfold (octagonal), tenfold (decagonal), and twelvefold (dodecagonal) symmetry axes.[1] A central problem in condensed-matter physics is to determine whether quasiperiodicity leads to new physical properties which are significantly different from those of crystalline and amorphous materials.

The first few years of studies of QC's revealed that their physical properties are similar to either the corresponding crystalline or the amorphous counterparts.[1,2] It was only later realized that the first QC's, which were thermodynamically *metastable*, possessed significant structural disorder, as manifested in the broadening of x-ray and/or electron diffraction lines. In addition, they contained non-negligible amounts of second phases. These poor-quality samples hampered the detection of those properties which were intrinsic to quasiperiodicity. They also led to confusion, especially in the area of magnetism of QC's where some "unusual" magnetic properties were claimed to have been observed.[3] Some of these properties were later shown[4] to result from the presence of magnetic second phases in the studied icosahedral (i) alloys.

A new impetus to studying the intrinsic properties due to quasiperiodicity came with the discovery of thermodynamically *stable* QC's.[1,2] These new QC's possess a high degree of structural perfection comparable to that found in the best periodic alloys.[1,2,5] Some unusual physical properties have been found in the most intensively studied i-alloys.[2] Their most striking feature, which is not expected for alloys consisting of normal metallic elements, is the very high value of the electrical resistivity (up to 2 Ω cm in the i-Al-Pd-Re system).[6,7] This corresponds to an electrical conductivity comparable to or smaller than the Mott's "minimum metallic conductivity" of 200 $\Omega^{-1}\,\mathrm{cm}^{-1}$ for the metal-insulator transition.[8] It was even suggested[7] that i-Al-Pd-Re is an insulator at low temperatures. The temperature coefficient of resistivity of these new i-alloys is generally negative,[1,2,6,7] which is inconsistent with the expected behavior for metals. Additionally, the resistivity is extremely sensitive to sample composition,[6,7] which is reminiscent of doping effects in semiconductors. Furthermore, the resistivity of these new i-alloys increases as their structural quality improves (by annealing which removes the defects),[2,6,7] in contrast to the behavior of typical metals. Other unexpected anomalies in the transport properties of i-alloys involve a very low electronic contribution to the specific heat, large and strongly temperature-dependent Hall coefficients and thermoelectric power, and a non-Drude-like optical conductivity.[1,2,6,7] From a magnetic point of view, the stable i-alloys of high structural quality are unusual in that they are diamagnetic[9] in spite of containing sig-

nificant concentrations of transition-metal (TM) atoms.

The physical properties of *i*-alloys mentioned above have been interpreted qualitatively almost exclusively in terms of a Hume-Rothery mechanism, which implies the existence of a pseudogap in the electronic density of states (DOS) in the vicinity of the Fermi level, E_F; this is in spite of some doubts about the theoretical justification of this mechanism for QC's.[10] Such an interpretation seems to be supported by the electronic structure calculations performed for the crystalline approximants of *i*-alloys;[11,12] these calculations predict a structure-induced pseudogap, or rather several pseudogaps, in the DOS around E_F. Spectroscopic data based on soft x-ray emission and absorption spectroscopies have been interpreted[13] as direct evidence for the existence of such a pseudogap, in spite of the limitations of the energy resolution used in comparison with the widths of the gaps and the severe lifetime broadening effects inherent to these techniques.[14]

There is another mechanism[10,15] which claims to give a good explanation of the electronic transport properties of *i*-alloys and which avoids some problems associated with extending the Hume-Rothery argument to alloys with TM elements. It is based on an internal structural model which assumes the presence of the conductive *i*-blocks which are enveloped by an insulating layered-structure network. For this structural model the electrical conduction occurs via tunneling.[10,15] Other mechanisms invoked to explain the electronic transport properties of *i*-alloys are based on the intraband transitions via electron hopping descriptions,[16] on the criticality of the wave functions,[17] or on a description of QC's as a hierarchy of clusters.[18] It is unclear at present what mechanisms are responsible for the unusual transport properties of *i*-alloys and to what extent these properties can be associated with the quasiperiodicity.

QC's of decagonal (*D*) symmetry combine two structural characteristics: The atoms are ordered quasiperiodically in planes which are stacked with translational periodicity. They represent thus an intermediate state between *i* and crystalline phases. The first stable *D*-alloys were discovered in the ternary Al-Co-Cu and Al-Co-Ni systems.[19,20] Samples of high structural quality can be produced in these two *D*-systems, which are therefore among the most intensively studied *D*-alloys. Most of the studies of *D*-alloys Al-Co-Cu and Al-Co-Ni are associated with their various structural aspects.[21] A few physical measurements which have been carried on these two *D*-alloys showed that, as expected, the electrical resistivity has metallic characteristics along the periodic direction, and exhibits a nonmetallic behavior, similar to that observed in *i*-alloys, in the quasiperiodic plane.[22–27] Anisotropies in the Hall effect,[26,28,29] thermopower,[22] thermal conductivity,[30] and optical conductivity[31] have also been observed. These two *D*-alloys were also shown to be diamagnetic over a wide temperature range.[32]

As is the situation for *i*-alloys, the physical properties of *D*-alloys have been interpreted qualitatively mainly by invoking the Hume-Rothery mechanism.[26,27,29,32] However, recent optical conductivity data[31] could not be reconciled with the existence of the pseudogap near E_F. This seems to be in agreement with the conclusion of a recent theoretical free-electron plane-wave model study[33] which showed that the periodicity in the tenfold direction removes or substantially suppresses the gap at E_F in *D*-alloys. On the other hand, the recent band-structure calculations[34] of an approximant $Al_{66}Co_{14}Cu_{30}$ of a *D*-alloy Al-Co-Cu predict the existence of a well-pronounced and very wide pseudogap at E_F. The width of this pseudogap in the occupied DOS is about 1 eV, and should therefore be seen directly in photoemission spectroscopy (PES) experiments of medium energy resolution (around 0.4 eV). It should be noted that this is in contrast to the situation for *i*-alloys where the center of the pseudogap is predicted to be located above E_F,[11,12] and thus the detection of its narrow width (<0.1 eV) below E_F is possible only by using high-energy-resolution spectroscopic techniques; such high-energy-resolution experiments have not been carried out yet.

In this paper we report the first investigation of the valence bands of two *D*-alloys $Al_{65}Co_{15}Cu_{20}$ and $Al_{70}Co_{15}Ni_{15}$. We identify the features of *d* character in the valence bands and show that, within the resolution of the experiment, there is no pseudogap in the *d*-character DOS below E_F in the studied alloys. The consequences of our experimental results are discussed.

II. EXPERIMENTAL PROCEDURE

Ingots of nominal compositions $Al_{65}Co_{15}Cu_{20}$ and $Al_{70}Co_{15}Ni_{15}$ were prepared by melting high-purity source metals in an argon atmosphere using an arc furnace. The ingots were annealed in vacuum as described elsewhere.[20] X-ray diffraction and electron microscopy studies showed that the samples are single phase and exhibit resolution-limited Bragg-peak widths.

Photoemission spectra were collected at room temperature on beam line U14A at the National Synchrotron Light Source at the Brookhaven National Laboratory. Photon energies $h\nu$ between 35 and 120 eV were selected with a plane grating monochromator. The normal to the sample was at an angle 45° to both the photon beam and the axis of a PHI 15-255 precision electron-energy analyzer. The resulting overall resolution was about 0.4 eV. The samples were cleaned in the experimental vacuum chamber by gentle mechanical abrasion using an alumina scraper. The surface cleanliness of the samples was frequently verified by monitoring the appearance of the oxide features in the PES spectra of the Al $2p$ core-level lines and/or of the valence bands.[35] The base pressure in the experimental chamber was in the high-10^{-11}-Torr range.

All the spectra presented here were obtained from at least two different regions of the samples studied, and were indistinguishable within the resolution of the experiment. The position of the Fermi level was determined with an accuracy of 0.05 eV by measuring the Fermi edge of an adjacent Al foil electrically connected to the samples.

III. RESULTS AND DISCUSSION

A. Methodology of the correction of the raw photoemission spectra

In order to compare in a meaningful way the intensities of the synchrotron-radiation-based PES spectra of a given sample, several corrections have to be taken into account. First, all PES spectra presented here were corrected for the energy dependence of the electron transmission of the electron-energy analyzer. It was assumed that the transmission of the analyzer is inversly proportional to the kinetic energy of the electrons.[36] Next, the PES spectra were normalized to the time-dependent photon flux. The secondary-electron contribution was then subtracted by using the Shirley method[37] in which the secondary-electron background intensity at each binding energy (BE) is assumed to be proportional to the total integrated signal at lower binding energies. The first two corrections slightly modify the shape of the raw spectrum, whereas the background subtraction causes the largest change (Fig. 1). These corrected spectra can be compared not only with respect to their shape but also in terms of their intensities.

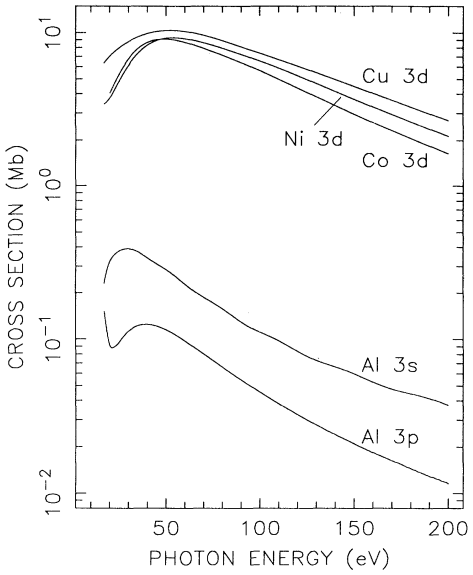

FIG. 2. Atomic subshell photoionization cross sections as a function of photon energy for different orbitals. Data are taken from Ref. 38. Note the logarithmic scale on the ordinate axis.

B. Resonant photoemission data

The two broad features in the valence band of $Al_{65}Co_{15}Cu_{20}$ (Fig. 1) must be predominantly due to the Co and Cu $3d$-derived states because the relatively small photoionization cross section σ for Al sp orbitals for the $h\nu$ values used here (Fig. 2) reduces significantly the Al sp contribution to the valence band. In order to identify the origin of these two features, photoemission spectra were measured for different values of $h\nu$.

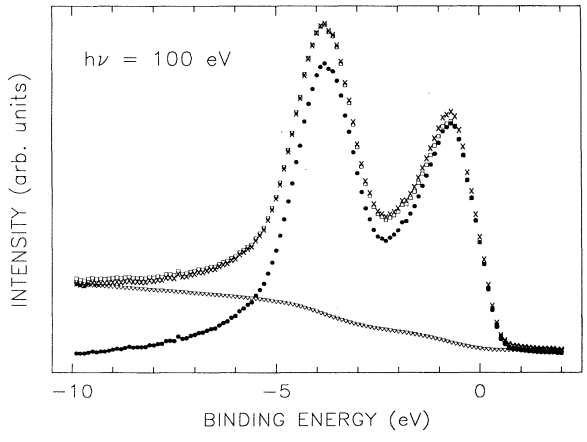

FIG. 1. Effect of various corrections on the valence-band spectrum of D-$Al_{65}Co_{15}Cu_{20}$ measured at a photon energy $h\nu$=100 eV. (□) the as-measured spectrum, (×) the analyzer- and flux-corrected as-measured spectrum which was scaled to the most intense peak of the as-measured spectrum, (▽) the secondary-electron contribution to the analyzer- and flux-corrected spectrum, and (•) the resultant spectrum after subtraction of the secondary-electron contribution.

Resonant photoemission is a particularly useful technique for determining the origin of atom-specific features in a valence band of an alloy.[39] It is based on an enhancement of an ionization cross section of an outer-shell electron as the excitation energy exceeds the threshold of an inner excitation. For TM atoms the resonance takes place at excitation energies near the $3p$ threshold, which for the Co $3p \rightarrow 3d$ transition used here is expected to occur at $h\nu \approx 59$ eV.[40] For a TM atom with a ground state configuration $3d^n$, resonance photoemission involves two processes. The first one is a direct excitation from the occupied valence band

$$3p^6 3d^n + h\nu \rightarrow 3p^6 3d^{n-1}\epsilon_f, \tag{1}$$

where ϵ_f labels the state of a photoelectron to be detected. The other involves a $3p$ electron being excited into an unoccupied $3d$ state which decays through an autoionization process where one $3d$ electron falls back to fill the $3p$ hole, thus transferring all its energy to a second electron which is emitted from the atom,

$$3p^6 3d^n + h\nu \rightarrow 3p^5 3d^{n+1} \rightarrow 3p^6 3d^{n-1}\epsilon_f. \tag{2}$$

Since the final state in Eq. (1) is identical to that in Eq. (2), there is a quantum interference between the two processes. Thus, when $h\nu$ is swept through the Co $3p \rightarrow 3d$ threshold the TM $3d$-derived features resonate; i.e., they are enhanced or suppressed.

It can be seen in Fig. 3 that, as $h\nu$ increases, the rela-

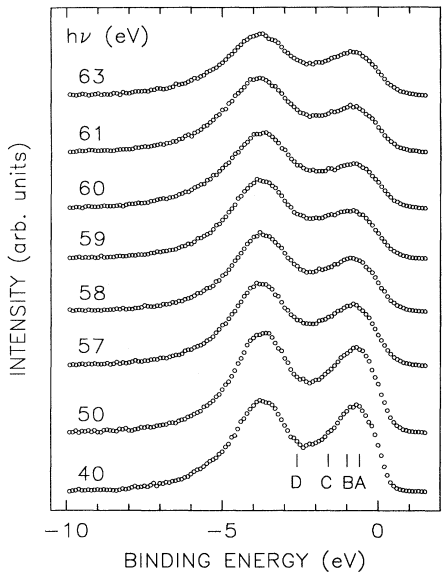

FIG. 3. Valence bands of D-$Al_{65}Co_{15}Cu_{20}$ measured for different photon energies around the Co $3p \rightarrow 3d$ transition. A, B, C, and D identify positions for which CIS spectra were measured (Fig. 5).

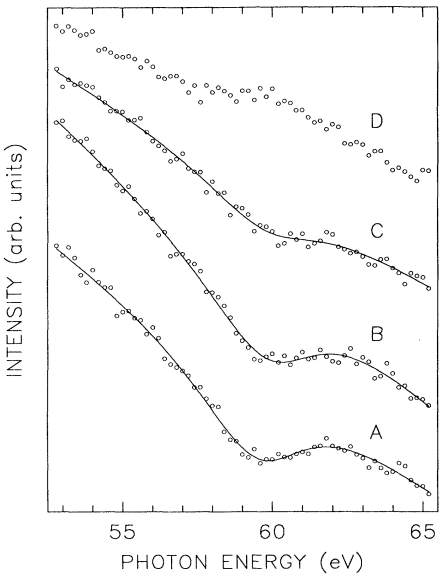

FIG. 5. CIS spectra measured for the valence band positions A, B, C, and D in Fig. 3, which are identified here by the same letters. The solid line is a fit to a Fano profile and a linear background [Eq. (3)] with parameters given in Table I.

tive intensity of the peak at BE≈−0.7 eV with respect to the peak at BE≈−3.7 eV decreases first, reaches its minimum at $h\nu$=60 eV, and then starts to increase for higher values of $h\nu$. Since in the vicinity of the Co $3p \rightarrow$3d transition the changes of σ with $h\nu$ are very small (Fig. 2), the suppression of the BE=−0.7 eV feature at $h\nu$=60 eV indicates that it is mainly of the Co $3d$ character.

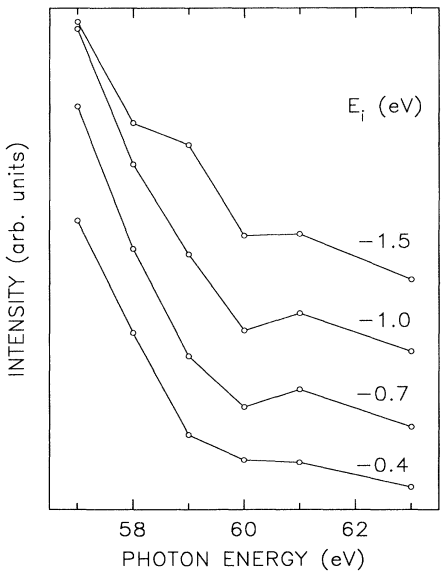

FIG. 4. CIS spectra for the indicated values of the initial energies which were calculated from the PES spectra in Fig. 3, as described in the text. The solid lines are guides for the eye.

A resonance photoemission experiment can be performed in the so-called constant-initial-state (CIS) mode, which shows more clearly the photoemission intensity variations due to resonance. The CIS spectra represent the dependence of the photoemission intensity on $h\nu$ for selected valence-band positions identified by their initial energy E_i. They can be obtained with two methods. The first method involves generating the CIS spectra directly from the valence-band spectra measured for different $h\nu$. Such CIS spectra obtained from the valence bands in Fig. 3 by plotting the intensity at a given BE versus $h\nu$ are shown in Fig. 4. The CIS intensity was calculated as an average of five PES intensity values around a given E_i in order to diminish possible CIS intensity fluctuations due to statistical uncertainties in the measured PES intensity. One can observe (Fig. 4) that the resonance occurs for $h\nu$ values around 60 eV and that it is strongest for the E_i values between −0.7 and −1.0 eV, which corresponds to the peak position of one of the two features in the PES spectra (Fig. 3). This confirms that the feature in Fig. 3 close to E_F is predominantly of the Co $3d$ character.

TABLE I. Parameters obtained by fitting the CIS spectra in Fig. 5 to the Fano line shape (3) for the E_i values corresponding to the positions A, B, and C indicated in Fig. 3.

E_i (eV)	I_0	E_R (eV)	q	Γ (eV)
−0.6	86(3)	59.7(2)	0.22(7)	4.6(3)
−1.0	84(4)	60.2(2)	0.31(9)	4.7(3)
−1.6	43(4)	60.0(5)	0.17(2)	4.7(6)

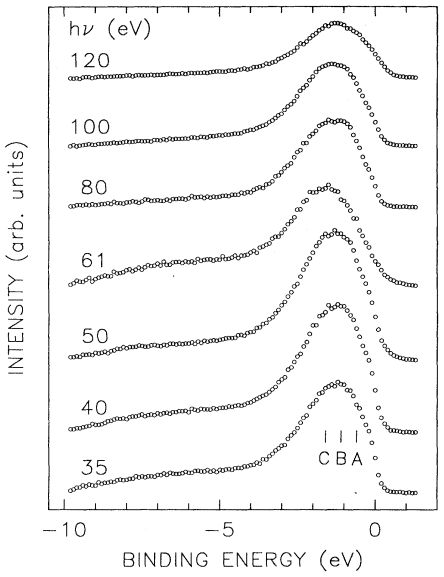

FIG. 6. Valence bands of D-$Al_{70}Co_{15}Ni_{15}$ measured for different photon energies. A, B, and C identify positions for which CIS spectra were measured (Fig. 7).

The generated CIS spectra (Fig. 4) consist of a small number of the experimental points (determined by the number of the PES spectra measured for different values of $h\nu$) and therefore do not lend themselves to a more quantitative analysis. The CIS spectra can be measured by a synchronous scanning of the photon and the electron kinetic energies. Such CIS spectra for the E_i values corresponding to the positions denoted by A, B, C, and

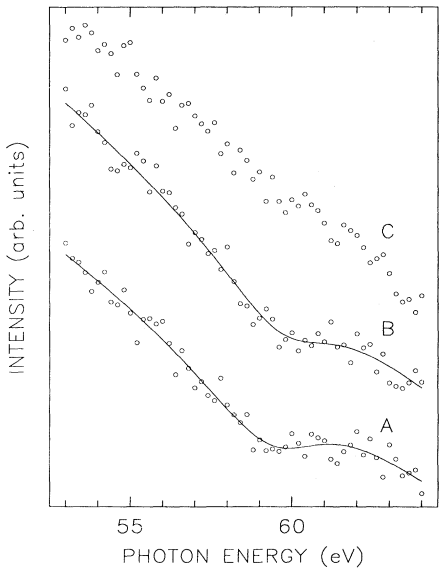

FIG. 7. CIS spectra measured for the valence band positions A, B, and C in Fig. 6, which are identified here by the same letters. The solid line is a fit to a Fano profile and a linear background [Eq. (3)] with parameters given in Table II.

TABLE II. Parameters obtained by fitting the CIS spectra in Fig. 7 to the Fano line shape (3) for the E_i values corresponding to the positions A and B indicated in Fig. 6.

E_i (eV)	I_0	E_R (eV)	q	Γ (eV)
−0.6	67(10)	59.7(7)	0.34(29)	4.6(9)
−1.1	66(6)	59.9(9)	0.22(9)	4.5(9)

D in Fig. 3 are shown in Fig. 5. One can clearly see a minimum for $h\nu$ around 60 eV. The line shape of the resonance resulting from the processes described by Eqs. (1) and (2), $I(h\nu)$, can be characterized by the Fano profile[39]

$$I(h\nu) = I_0(h\nu)\frac{(\epsilon+q)^2}{1+\epsilon^2} + I_{nr}(h\nu), \tag{3}$$

where $I_0(h\nu)$ is the nonresonant Co $3d$ emission, $I_{nr}(h\nu)$ is a noninterfering background contribution, q is Fano's asymmetry parameter, and $\epsilon = 2(h\nu - E_R)/\Gamma$ is the reduced energy expressed in terms of the energy E_R and width Γ [full width at half maximum (FWHM)] of the resonance. A linear background $I_{nr}(h\nu)$ was assumed in the fit. The parameters obtained from the fit are given in Table I.

Even though a good fit of the CIS spectra was obtained (Fig. 5), the fitted parameters are correlated and therefore caution is required in their physical interpretation. The E_R values (Table I) are close to the corresponding BE value of the Co $3p$ core level.[40] A relatively broad character of the resonance is reflected in the large value of Γ. The strongest resonance occurs between E_i=−0.6 eV and E_i=−1.0 eV and it extends up to E_i=−1.6 eV. The fact that the resonance takes place in a rather broad BE region can be interpreted as evidence of hybrydization between the Co $3d$ and the Al sp and/or Cu $3d$ states. We conclude that the peaks at BE=−0.7 and −3.7 eV in the valence band of D-$Al_{65}Co_{15}Cu_{20}$ (Fig. 3) are, respectively, due to the Co $3d$ and Cu $3d$ states.

The main broad feature in the valence band of D-$Al_{70}Co_{15}Ni_{15}$ (Fig. 6) must result from a strong overlap of the Co $3d$ and Ni $3d$ states. The contribution to this feature due to the Co $3p$ states has been verified by measuring the CIS spectra (Fig. 7) which were fitted in the same way as descibed above. The values of the fitted parameters of the CIS spectra of D-$Al_{70}Co_{15}Ni_{15}$ (Table II) are similar to the corresponding values for D-$Al_{65}Co_{15}Cu_{20}$ (Table I). It can be noticed, in particular, that no resonance is observed for E_i=−1.6 eV for D-$Al_{70}Co_{15}Ni_{15}$ (plot C in Fig. 7), whereas for the same E_i value a resonance occurs for D-$Al_{65}Co_{15}Cu_{20}$ (plot C in Fig. 5). This indicates that the Co $3d$ states are strongly hybridized with the Ni $3d$ and/or Al sp states in D-$Al_{70}Co_{15}Ni_{15}$.

C. Partial DOS due to Co 3d- and Cu 3d-derived states

It is now widely accepted that PES valence bands measured typically for hν $\geq$40 eV represent the initial DOS weighted by frequency-dependent dipole matrix elements

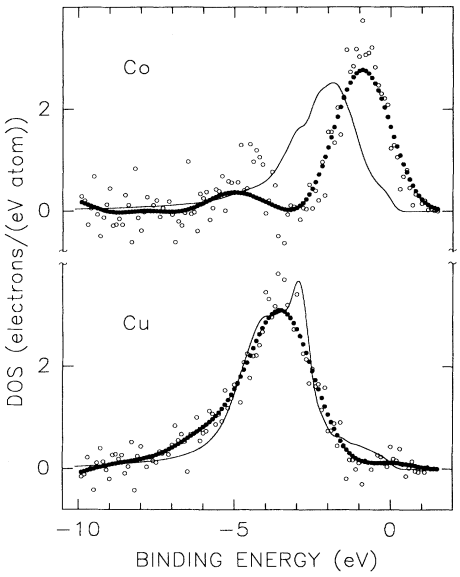

FIG. 8. Partial DOS of the Co and Cu 3*d* states in *D*-$Al_{65}Co_{15}Cu_{20}$ (○) obtained from the $h\nu$=60 eV and 63 eV valence bands in Fig. 3, and later smoothed (●). The broadened theoretical DOS (solid line) is from Ref. 34, as described in the text.

and by the $\sigma(h\nu)$ values for various *s*, *p*, *d*, and *f* states.[41] To a good approximation, it can be assumed that the matrix elements do not change significantly over the width of the valence bands. Thus the measured PES valence bands, when corrected for experimental factors and for inelastically scattered electrons, are generally proportional to the DOS modulated by the σ values. Before the availability of synchrotron radiation as a tunable excitation source, the *partial* spectral weights due to *d* or *f* states of a given element in an alloy, which are generally proportional to the partial DOS associated with a given state of that element, were determined almost exclusively using the soft x-ray emission technique. The use of synchrotron-radiation-based PES allows one also to determine partial DOS for some orbitals.[42]

By taking the difference between the on- ($h\nu$=63 eV) and off-resonance ($h\nu$=60 eV) valence bands in Fig. 3, which have been scaled either to the height of the Cu 3*d* peak or to the height of the Co 3*d* peak, one obtains respectively the partial DOS of the Co 3*d* and Cu 3*d* character (open circles in Fig. 8); these partial DOS have been normalized to the corresponding number of 3*d* electrons per atom. As the difference spectra had a large scatter, they were smoothed (solid circles in Fig. 8) to allow a better comparison with the theoretical partial Co and Cu 3*d* DOS.[34]

D. Minimum of DOS(E_F)

In a recent study the electronic structure of the hypothetical approximant $Al_{60}Co_{14}Cu_{30}$ of a *D*-alloy Al-Co-Cu has been calculated.[34] The theoretical DOS, which was kindly provided to us by T. Fujiwara, exhibits a well pronounced pseudogap at E_F.[34] In order to make a meaningful comparison between the theoretical and experimental partial DOS, the former has to be appropriately broadened to account for the lifetime broadening effects inherent to the PES technique and for the finite resolution of a PES experiment. The theoretical Co 3*d* and Cu 3*d* DOS were first multiplied by the Fermi-Dirac function at room temperature, then convoluted with a Lorentzian to account for the lifetime broadening, and finally convoluted with a Gaussian to account for the instrumental broadening. The Lorentzian FWHM was taken in the form $\Gamma_L^0(|BE| - E_F)^2$ (Ref. 43) which is predicted by Fermi liquid theory.[44] The Γ_L^0 parameter, which fixes the scale of the broadening, was chosen to be 0.02 eV^{-1} since for this value one obtains good agreement between the theoretical and experimental widths of the Cu 3*d* DOS. The Gaussian FWHM was 0.4 eV. As can be seen from Fig. 8, there is a striking disagreement between the theoretical and experimental Co 3*d* DOS. In contrast to the theoretical prediction of a pronounced Hume-Rothery pseudogap at E_F in the Co 3*d* DOS,[34] no such pseudogap can be seen in the experimental Co 3*d* DOS (Fig. 8). In fact, there is a significant experimental Co 3*d* DOS at E_F, which can be also clearly seen in the valence bands (Fig. 3).

In order to compare the theoretical PES valence band resulting from the total theoretical DOS (Ref. 34) of an approximant of the *D*-alloy with the PES valence band measured at $h\nu$=100 eV, the theoretical partial Al, Co, and Cu DOS associated with different angular momenta[34] were first multiplied by the corresponding σ values[38] and normalized for the number of corresponding electrons in the valence band.[45] Their sum (Fig. 9), which differs only slightly from the total theoretical DOS of an approximant of the *D*-alloy,[34] represents the theoretical

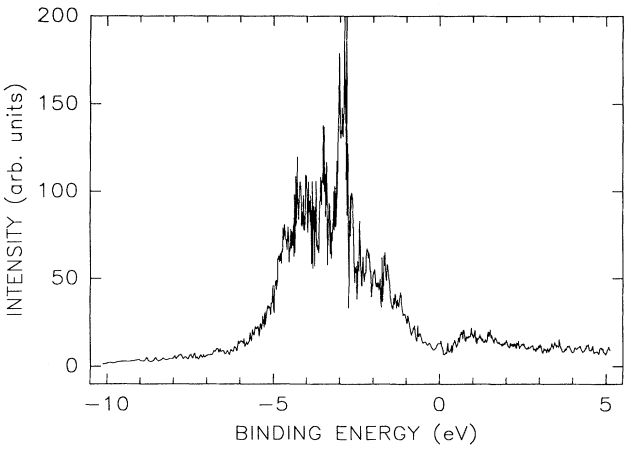

FIG. 9. Theoretical $h\nu$=100 eV PES valence band of a *D*-Al-Co-Cu alloy which was obtained by summing the theoretical partial Al, Co, and Cu DOS associated with different angular momenta from Ref. 34 weighted by the corresponding σ values from Ref. 38 and by the composition and the number of electrons (Ref. 45).

PES valence band which would be expected in a hypothetical PES experiment with an infinitely high energy resolution and no lifetime broadening effects. A distinct and wide pseudogap at E_F (Fig. 9) is predicted.[34]

The theoretical PES valence band in Fig. 9 was next broadened in the same way as described above and compared with the valence band of D-$Al_{65}Co_{15}Cu_{20}$ measured at $h\nu$=100 eV (Fig. 10). A wide pseudogap at E_F predicted by theory[34] is clearly not present in the experimental valence band (Fig. 10). Furthermore, even by allowing for the difference in composition between the approximant $Al_{66}Co_{14}Cu_{30}$ and D-$Al_{65}Co_{15}Cu_{20}$, the theoretical Co 3d spectral weight is much smaller than observed experimentally (Fig. 10).

The main feature in the valence band of D-$Al_{70}Co_{15}Ni_{15}$ (Fig. 6) results from a strong overlap of the Co 3d and Ni 3d states. Because of this overlap, it was not possible to separate the partial DOS associated with the Co and Ni 3d states. No electronic structure calculations have been performed yet for an approximant of this D-alloy. However, a comparison of the valence bands of D-$Al_{65}Co_{15}Cu_{20}$ and D-$Al_{70}Co_{15}Ni_{15}$ (Fig. 11) shows that there is also no pseudogap at E_F in D-$Al_{70}Co_{15}Ni_{15}$, as in the case of D-$Al_{65}Co_{15}Cu_{20}$. It can be also noticed that the area under the valence bands (Fig. 6) decreases with increasing $h\nu$, in accordance with the corresponding change of σ values (Fig. 2).

It is useful to compare the valence bands of D-$Al_{65}Co_{15}Cu_{20}$ and D-$Al_{70}Co_{15}Ni_{15}$ with the valence bands of their constituent elements (Fig. 12). A clear shift of the Cu 3d spectral weight in D-$Al_{65}Co_{15}Cu_{20}$ away from E_F as compared with the corresponding spectral weight in pure Cu can be noticed (Fig. 12). Such a shift is expected to result in a decrease of the Cu 3d contribution to the DOS(E_F). A similar shift is not observed for the Co and Ni 3d spectral weights (Fig. 12) and consequently one can anticipate a non-negligible contribution of the Co and Ni 3d-like states to the DOS(E_F)

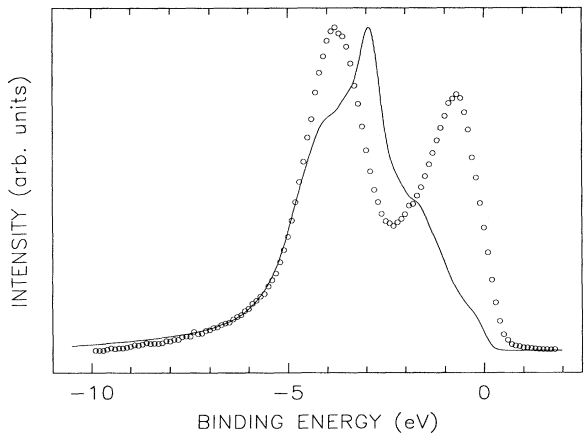

FIG. 10. Comparison between the valence band of D-$Al_{65}Co_{15}Cu_{20}$ measured at $h\nu$=100 eV (○) and the broadened theoretical PES valence band (solid line) from Fig. 9, as described in the text.

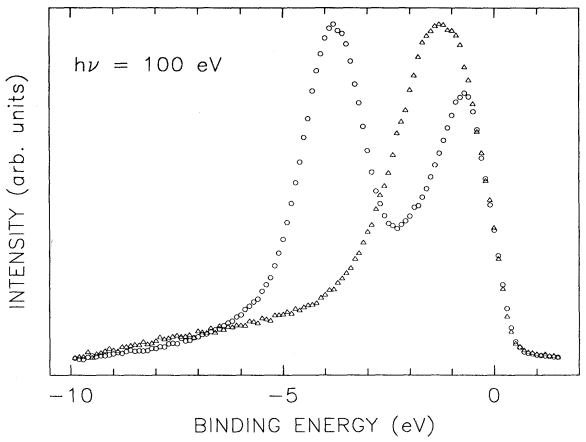

FIG. 11. Comparison of valence bands of D-alloys $Al_{65}Co_{15}Cu_{20}$ (○) and $Al_{70}Co_{15}Ni_{15}$ (△) measured at $h\nu$=100 eV.

for the D-$Al_{65}Co_{15}Cu_{20}$ and D-$Al_{70}Co_{15}Ni_{15}$ alloys. The Al sp states are expected to spread throughout the valence bands of D-$Al_{65}Co_{15}Cu_{20}$ and D-$Al_{70}Co_{15}Ni_{15}$, but cannot be detected clearly in the measured spectra due to the small σ values associated with the Al s and p orbitals (Fig. 2). These states contribute to a broad

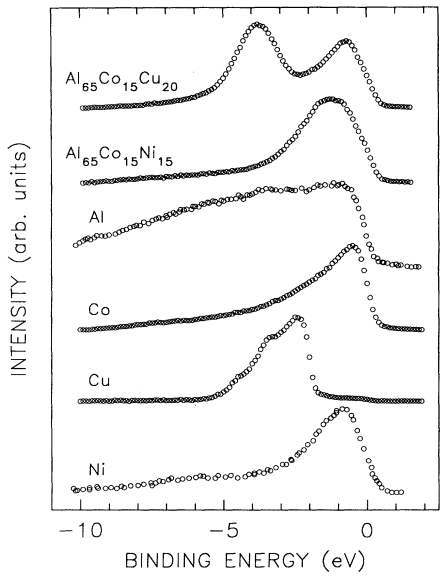

FIG. 12. Comparison of valence bands of D-alloys $Al_{65}Co_{15}Cu_{20}$ and $Al_{70}Co_{15}Ni_{15}$ with the valence bands of Al (Fig. 2 in Ref. 46), Co, Cu (the raw PES spectrum was kindly provided by T.-U. Nahm and S.-J. Oh; the secondary-electron contribution was subtracted from the original spectrum), and Ni [Fig. 4(a) in Ref. 47; the secondary-electron contribution was subtracted from the original spectrum] metals. All valence bands were measured at $h\nu$=100 eV except for the valence band of the Al metal which was measured with Mg $K\alpha$ radiation (1253.6 eV). The spectra were normalized to give a constant height between the maximum and minimum recorded count.

spectral weight below BE=−6 eV where the contributions from the Co, Cu, and Ni 3*d*-derived states are relatively small. This spectral weight could be also caused by surface oxidation,[35] but this possibility can be excluded as the surface cleanliness was carefully monitored during the PES experiments. We conclude that the PES data presented here are conclusive evidence for the lack of a pseudogap at E_F in two *D*-alloys of high structural quality. This can be interpreted as evidence that the Hume-Rothery mechanism does not play an important role in the stability and transport properties of *D*-alloys. This finding agrees with the suggestion based on the results of the recent optical conductivity[31] and the plane-wave model[33] studies, and is at variance with the interpretation of the electronic transport data[26,27,29,32] and the prediction based on the energy-band calculations.[34]

The lack of a pseudogap at E_F in *D*-alloys means that there is a fundamental difference between their electronic structure and that of *i*-alloys in which this pseudogap seems to exist.[1,2,11–13] Therefore, one has to consider other unconventional mechanisms to account for the unusual physical properties of *D*-alloys.

E. Fine strucure of DOS

The notion of a structure-induced pseudogap, which is theoretically predicted for both *i* (Refs. 11, 12) and *D* (Ref. 34) alloys, but which seems to be realized only in *i*-alloys,[1,2,13] is believed to be a *generic* property of QC's. It is not, however, a *specific* property distinguishing QC's from the periodic or aperiodic phases because such a pseudogap was shown to be also present in some amorphous[48] or crystalline[49] materials. A property which, according to some electronic structure calculations,[11,12,34] is specific only to QC's is the fine structure (spikiness) of their DOS (Fig. 9) resulting from a large number of nondegenerated flat bands. Although such spikiness is predicted to be attenuated[34] in the *D*-Al-Co-Cu alloys in comparison to the *i*-alloys by the effect of the periodic direction, it is still clearly visible, especially in the vicinity of the Cu 3*d* peak (Fig. 9).[34] The width of a spiky peak is predicted[11,34] to be of the order of 0.01–0.02 eV. The valence bands of the *D*-alloys $Al_{65}Co_{15}Cu_{20}$ and $Al_{70}Co_{15}Ni_{15}$ presented here show no evidence for the presence of such spikes. These spikes have also not been detected directly in other spectroscopic measurements of QC's.[5,13,14,35]

There are several possible explanations of the failure to detect these spikes in experiment (provided that they indeed exist). Assuming a hypothetical case of a PES experiment with no lifetime broadening, an energy resolution better than about 0.1 eV is required (left panel of Fig. 13) to detect the spikes. In a real PES experiment, lifetime broadening effects are present (Sec. III D) and they smear out even further (especially far from E_F) the fine features in the DOS (right panel of Fig. 13). It can be concluded that the predicted[34] DOS spikiness can be observed with the PES experiments of the highest energy resolution ($\lesssim$20 meV), and *only in the vicinity of* E_F. Such PES experiments have not been performed yet. Soft x-ray emission spectroscopy is not suitable for detecting such spikes because of much more severe broadening effects[14] around E_F inherent to this technique.

It may not be possible to detect the predicted DOS spikiness even with the PES experiments of the highest energy resolution because of the existence of chemical and topological disorder in QC's of high structural quality. Such disorder, which is not taken into account in the electronic structure calculations, may wash out the DOS spikiness induced by quasiperiodicity. All known

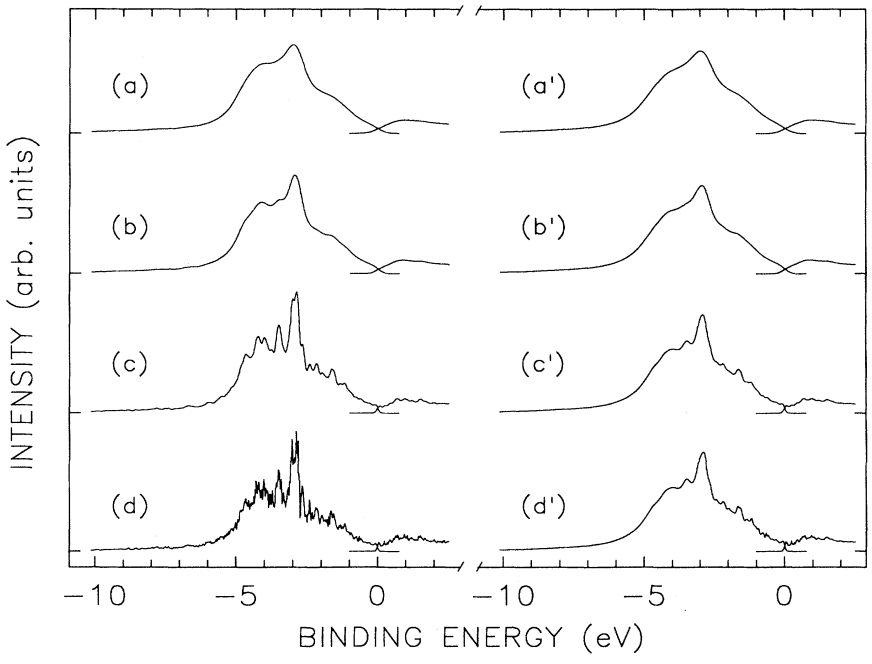

FIG. 13. Left panel: theoretical PES spectrum from Fig. 9 multiplied by the Fermi-Dirac distribution function at room temperature and convoluted with a Gaussian of the FWHM equal to (a) 0.6, (b) 0.4, (c) 0.1, and (d) 0.02 eV. Right panel: theoretical PES spectrum from Fig. 9 multiplied by the Fermi-Dirac distribution function at room temperature and convoluted with a Lorentzian of the FWHM equal to $\Gamma_L^0(|BE| - E_F)^2$, where Γ_L^0=0.02 eV^{-1}, and with a Gaussian of the FWHM equal to (a') 0.6, (b') 0.4, (c') 0.1, and (d') 0.02 eV.

stable QC's are ternary alloys and most of them are based on aluminum. If one envisages that their structure consists of an *sp*-electron-type sublattice and a *d*-electron-type sublattice, then clearly one expects the presence of chemical disorder in these sublattices (for example, in the CoCu and CoNi sublattices of the *D*-alloys studied here). Furthermore, the concept of quasiperiodicity implies that no two crystallographic positions of a given atom are exactly the same,[50] which can be viewed as a sort of topological disorder.

Although the two types of disorder mentioned above are not seen in the diffraction and electron microscopy experiments on "perfect" (phason-free) QC's, there is growing experimental evidence based on other experimental techniques which shows that chemical and topological disorder are present in these structurally perfect QC's. For example, local probes such as Mössaber spectroscopy,[4,51,52] NMR,[53] and nuclear quadrupole resonance (NQR) (Ref. 53, 54) clearly detect the distribution of the electric quadrupole splittings in high-quality stable QC's. Such a distribution can be detected only if there is a chemical and/or topological disorder in the investigated samples. A recent study on the propagation of acoustic waves in a single-grain *i*-Al-Pd-Mn sample shows the similarity of the acoustic properties of this alloy to those of amorphous metals.[55] The apparent success of quantum interference theories (the electron-electron interaction and weak-localization effects),[1,2] which were originally developed for highly disordered conductors, in accounting for the temperature and field dependences of the electrical conductivity and magnetoresistance of high-quality QC's also indicates the importance of chemical disorder (topological disorder produced by quasiperiodicity cannot be directly associated with these theories because they start with Bloch waves and perturb them with disorder, whereas wave functions in QC's cannot be written as perturbed Bloch states). The experiments mentioned above[1,2,4,51–55] demonstrate that chemical and/or topological disorder is present also in the high-quality phason-free stable QC's and must be taken into account in attempts to understand the physical properties of QC's.

F. Al 2*p* chemical shift

The Al 2*p* core-level lines in Al metal and in *D*-alloys $Al_{65}Co_{15}Cu_{20}$ and $Al_{70}Co_{15}Ni_{15}$ are compared in Fig. 14. One can notice that the Al $2p_{1/2}$ and $2p_{3/2}$ lines are separated in the Al metal (inset in Fig. 14), but they overlap in the *D*-alloys. The separation of the Al $2p_{1/2}$ and $2p_{3/2}$ lines in the Al metal determined from a fit using the two Doniach-Šunjić profiles[56] convoluted with a Gaussian (inset in Fig. 14) is 0.41(1) eV, which is in a good agreement with the value of 0.42 eV reported in the literature.[57] The Gaussian FWHM obtained from the fit was 0.418(7) eV. This, together with the observation of the Al $2p_{1/2}$ and $2p_{3/2}$ components in the Al metal, confirms that the overall resolution of the recorded PES spectra is about 0.4 eV. The main result obtained from Fig. 14 is the observation of the BE shift of the Al 2*p* line

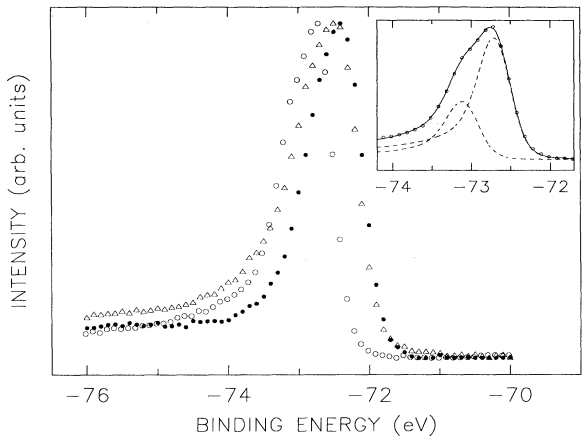

FIG. 14. Al 2*p* photoemission lines of the Al metal (○) and *D*-alloys $Al_{65}Co_{15}Cu_{20}$ (●) and $Al_{70}Co_{15}Ni_{15}$ (△) measured at $h\nu$=100 eV. The lines were normalized to give a constant height between the maximum and minimum recorded counts. The inset shows the fit (solid line) of the Al 2*p* line of the Al metal with two Doniach-Šunjić profiles corresponding to Al $2p_{1/2}$ and $2p_{3/2}$ core levels, which are also shown, convoluted with a Gaussian.

in the *D*-alloys $Al_{65}Co_{15}Cu_{20}$ and $Al_{70}Co_{15}Ni_{15}$, respectively, by 0.36(3) and 0.30(3) eV towards lower absolute BE values with respect to Al metal. There are only a few reports of shifts of the core-level lines in QC's with respect to pure elements and/or to other crystalline alloys. Ederer *et al.*[58] reported the chemical shifts of 0.2 eV between the Al-Mn alloys of different crystal structures and pure Al, and of less 0.1 eV between the Al-Mn alloys of crystalline and *i* structure. Matsubara *et al.*[59] found a 0.4 eV shift of the Al 2*p* and Li 1*s* lines towards higher absolute BE values in *i*-$Al_{55}Li_{35.8}Cu_{9.2}$ with respect to the Frank-Kasper crystalline alloy $Al_{54}Li_{36.8}Cu_{9.2}$. The absolute BE shift of the Al 2*p* line in *i*-$Al_{70}Pd_{20}Mn_{10}$ with respect to a pure Al metal reported by Zhang *et al.*[5] was 0.27(10) eV. The values of the observed shifts are small and are comparable to those observed in crystalline alloys.[60] The interpretation of the BE shift is complicated by the fact that it consists of contributions due to chemical, configuration, and relaxation shifts.[61] These contributions are difficult to evaluate theoretically even for simple binary alloys.[61]

IV. CONCLUSIONS

The structure of the valence band of *D*-$Al_{65}Co_{15}Cu_{20}$ consists of two main features with the maximum intensity at 0.7(2) and 3.7(1) eV below E_F. The first feature was shown to be due to the Co 3*d*-derived states, whereas the second feature originates from the Cu 3*d*-like states. The location of the feature associated with the Co 3*d*-derived states is the same in the valence band of *D*-$Al_{70}Co_{15}Ni_{15}$ and these states strongly overlap with the states of the Ni 3*d* character. Therefore these two states must be significantly hybridized. The TM 3*d*-like states are also hy-

bridized with the Al *sp* states in the two *D*-alloys. The weak spectral weight at about 6 eV below E_F observed in the valence bands of both alloys was ascribed to the Al *sp*-derived states.

The partial DOS of Co 3*d* and Cu 3*d* character were determined from the on- and off-resonance valence bands of *D*-$Al_{65}Co_{15}Cu_{20}$ and compared with the broadened theoretical partial DOS calculated for the approximant of this alloy. Also the valence band was compared with the broadened theoretical total DOS. These comparisons convincingly demonstrated that within the experimental resolution, contrary to the prediction of recent band-structure calculations, there is no pseudogap in the DOS at E_F in *D*-$Al_{65}Co_{15}Cu_{20}$. A similar conclusion was reached for *D*-$Al_{70}Co_{15}Ni_{15}$. A Hume-Rothery mechanism cannot therefore be invoked to explain the stability and transport properties of *D*-alloys.

The theoretically predicted spikiness in the DOS was not observed. It was shown that such spikiness, if it indeed exists, can be detected only in the vicinity of E_F by performing PES experiments with the highest possible energy resolution. The influence of the presence of chemical and topological disorder on the electronic structure of QC's of high structural quality was indicated.

ACKNOWLEDGMENTS

This work was supported by the Natural Sciences and Engineering Research Council of Canada and by the Ministry of Education, Science, and Culture of Japan. The research was carried out (in part) at the National Synchrotron Light Source, Brookhaven National Laboratory, which is supported by the U.S. Department of Energy, Division of Materials Sciences and Division of Chemical Sciences (DOE Contract No. DE-AC02-76-CH00016). Two of us (Z.M.S. and G.W.Z.) are indebted to Dr. M.-L. Shek for her help in conducting the PES experiments.

* Author to whom correspondence should be addressed.

[1] C. Janot, *Quasicrystals: A Primer* (Oxford University Press, New York, 1992); in *Quasicrystals, The State of the Art*, edited by D.P. DiVincenzo and P.J. Steinhardt (World Scientific, Singapore, 1991); in *Quasicrystals*, edited by T. Fujiwara and T. Ogawa (Springer-Verlag, Berlin, 1990).

[2] S. Takeuchi, Mater. Sci. Forum **150-151**, 35 (1994), and references therein; S.J. Poon, Adv. Phys. **41**, 303 (1992), and references therein.

[3] R.C. O'Handley, R.A. Dunlap, and M.E. McHenry, in *Handbook of Magnetic Materials*, edited by K.H.J. Buschow (Elsevier, Amsterdam, 1991), Vol. 6, p. 453.

[4] Z.M. Stadnik and G. Stroink, Phys. Rev. B **43**, 894 (1991); **44**, 4255 (1991); S. Nasu, M. Miglierini, and T. Kuwano, *ibid.* **45**, 12778 (1992).

[5] G.W. Zhang, Z.M. Stadnik, A.-P. Tsai, and A. Inoue, Phys. Rev. B **50**, 6696 (1994).

[6] H. Akiyama, Y. Honda, T. Hashimoto, K. Edagawa, and A. Takeuchi, Jpn. J. Appl. Phys. B **7**, L1003 (1993); Y. Honda, K. Edagawa, A. Yoshika, T. Hashimoto, and S. Takeuchi, Jpn. J. Appl. Phys. A **9**, 4929 (1994).

[7] F.S. Pierce, S.J. Poon, and Q. Guo, Science **261**, 737 (1993); C. Berger, T. Grenet, P. Lindqvist, P. Lanco, J.C. Grieco, G. Fourcaudot, and F. Cyrot-Lackmann, Solid State Commun. **87**, 977 (1993); F.S. Pierce, Q. Guo, and S.J. Poon, Phys. Rev. Lett. **73**, 2220 (1994).

[8] N. Mott, *Conduction in Non-Crystalline Materials* (Clarendon, Oxford, 1993).

[9] S. Matsuo, T. Ishimasa, H. Nakano, and Y. Fukano, J. Phys. F **18**, L175 (1988); Z.M. Stadnik, G. Stroink, H. Ma, and G. Williams, Phys. Rev. B **39**, 9797 (1989); T. Klein, C. Berger, D. Mayou, and F. Cyrot-Lackmann, Phys. Rev. Lett. **66**, 2907 (1991).

[10] J.C. Phillips, Phys. Rev. B **47**, 7747 (1993).

[11] G. Trambly de Laissardière and T. Fujiwara, Phys. Rev. B **50**, 5999 (1994), and references therein.

[12] M. Windisch, M. Krajčı, and J. Hafner, J. Phys. Condens. Matter **6**, 6977 (1994), and references therein.

[13] E. Belin, Z. Dankhazi, and A. Sadoc, Mater. Sci. Eng. A **181-182**, 717 (1994), and references therein.

[14] G.W. Zhang, Z.M. Stadnik, A.-P. Tsai, A. Inoue, and T. Miyazaki, Z. Phys. B **97**, 439 (1995).

[15] J.C. Phillips and K.M. Rabe, Phys. Rev. Lett. **66**, 923 (1991); J.C. Phillips, Solid State Commun. **83**, 379 (1992); Phys. Rev. B **47**, 2522 (1993).

[16] D. Mayou, C. Berger, F. Cyrot-Lackmann, T. Klein, and P. Lanco, Phys. Rev. Lett. **70**, 3915 (1993).

[17] H. Tsunetsugu, T. Fujiwara, K. Ueda, and T. Tokihiro, Phys. Rev. B **43**, 8879 (1991); B. Passaro, C. Sire, and V.G. Benza, *ibid.* **46**, 13 751 (1992).

[18] C. Janot and M. de Boissieu, Phys. Rev. Lett. **72**, 1674 (1994).

[19] L.X. He, Y.K. Wu, and K.H. Kuo, J. Mater. Sci. Lett. **7**, 1284 (1988).

[20] A.-P. Tsai, A. Inoue, and T. Masumoto, Mater. Trans. Jpn. Inst. Met. **30**, 300 (1989); *ibid.* **30**, 463 (1989); A.R. Kortan, F.A. Thiel, H.S. Chen, A.P. Tsai, A. Inoue, and T. Masumoto, Phys. Rev. B **40**, 9397 (1989).

[21] W. Steurer, Mater. Sci. Forum **150-151**, 15 (1994), and references therein.

[22] L. Shu-yuan, W. Xue-mei, L. Li, Z. Dian-lin, L.X. He, and K.X. Kuo, Phys. Rev. B **41**, 9625 (1990).

[23] T. Shibuya, T. Hashimoto, and S. Takeuchi, J. Phys. Soc. Jpn. **59**, 1917 (1990).

[24] S. Martin, A.F. Hebard, A.R. Kortan, and F.A. Thiel, Phys. Rev. Lett. **67**, 719 (1991).

[25] S. Takeuchi, H. Akiyama, N. Naito, T. Shibuya, T. Hashimoto, K. Edagawa, and K. Kimura, J. Non-Cryst. Solids **153-154**, 353 (1993).

[26] W. Yun-ping, L. Li, and Z. Dian-Lin, J. Non-Cryst. Solids **153-154**, 361 (1993).

[27] W. Yun-ping and Z. Dian-lin, Phys. Rev. B **49**, 13 204 (1994).

[28] Z. Dian-lin, L. Li, W. Xue-mei, L. Shu-yuan, L.X. He, and K.H. Kuo, Phys. Rev. B **41**, 8557 (1990).

[29] W. Yun-ping, Z. Dian-lin, and L.F. Chen, Phys. Rev. B **48**, 10 542 (1993).

[30] Z. Dian-lin, C. Shao-chun, W. Yun-ping, L. Li, W. Xue-mei, X.L. Ma, and K.H. Kuo, Phys. Rev. Lett. **66**, 2778 (1991).

[31] D.N. Basov, T. Timusk, F. Barakat, J. Greedan, and B. Gruschko, Phys. Rev. Lett. **72**, 1937 (1994).
[32] R. Lück and S. Kek, J. Non-Cryst. Solids **153-154**, 329 (1993).
[33] R.F. Sabiryanov and S.K. Bose, J. Phys. Condens. Matter **6**, 6197 (1994).
[34] G. Trambly de Laissardière and T. Fujiwara, Mater. Sci. Eng. A **181-182**, 722 (1994); Phys. Rev. B **50**, 9843 (1994).
[35] Z.M. Stadnik and G. Stroink, Phys. Rev. B **47**, 100 (1993).
[36] J.C. Helmer and N.H. Weichert, Appl. Phys. Lett. **13**, 266 (1968).
[37] D.A. Shirley, Phys. Rev. B **5**, 4709 (1972).
[38] J.-J. Yeh, *Atomic Calculation of Photoionization Cross-Sections and Asymmetry Parameters* (Gordon and Breach, New York, 1993).
[39] L.C. Davis, J. Appl. Phys. **59**, R25 (1986).
[40] J.C. Fuggle and N. Mårtensson, J. Electron Spectrosc. Relat. Phenom. **21**, 27 (1980).
[41] D.E. Eastman and W.D. Grobman, Phys. Rev. Lett. **28**, 1327 (1972); J. Freeouf, M. Erbudak, and D.E. Eastman, Solid State Commun. **13**, 771 (1973); D.E. Eastman, J. Freeouf, and M. Erbudak, J. Phys. (Paris) Colloq. **34**, C6-37 (1973); P.J. Feibelman and D.E. Eastman, Phys. Rev. B **10**, 4932 (1974).
[42] J.W. Allen, S.J. Oh, O. Gunnarsson, K. Schönhammer, M.B. Maple, M.S. Torikachvili, and I. Lindau, Adv. Phys. **35**, 275 (1986).
[43] H. Höchst, P. Steiner, G. Reiter, and S. Hüfner, Z. Phys. B **42**, 199 (1981).
[44] D. Pines and P. Noziers, *The Quantum Theory of Liquids* (W.A. Benjamin, New York, 1966), pp. 63 and 309; N.W. Ashcroft and N.D. Mermin, *Solid State Physics* (Saunders College, Philadelphia, 1976), p. 347.
[45] A. Goldmann, J. Tejada, N.J. Shevchik, and M. Cardona, Phys. Rev. B **10**, 4388 (1974); J. Tejada, N.J. Shevchik, W. Braun, A. Goldmann, and M. Cardona, *ibid.* **12**, 1557 (1975).
[46] Y. Baer and G. Busch, Phys. Rev. Lett. **30**, 280 (1973).
[47] M.F. López, C. Laubschat, A. Gutiérrez, A. Höhr, M. Domke, G. Kaindl, and M. Abbate, Z. Phys. B **95**, 9 (1994).
[48] P. Häussler, in *Glassy Metals III*, edited by H. Beck and H.-J. Güntherodt (Springer-Verlag, Berlin, 1994), p. 163.
[49] Y. Baer and H.P. Myers, Solid State Commun. **21**, 833 (1977); J.-M. Imer, F. Patthey, B. Dardel, W.-D. Schneider, Y. Baer, Y. Petroff, and A. Zettl, Phys. Rev. Lett. **62**, 336 (1989); B. Dardel, M. Grioni, D. Malterre, P. Weibel, Y. Baer, and F. Lévy, J. Phys. Condens. Matter **5**, 6111 (1993); K.E. Smith and V.E. Henrich, Phys. Rev. B **50**, 1382 (1994); M. Nakamura, A. Sekiyama, H. Namatame, H. Kino, A. Fujimori, A. Misu, H. Ikoma, M. Matoba, and S. Anzai, Phys. Rev. Lett. **73**, 2891 (1994).
[50] Ch. Janot and J.M. Dubois, J. Phys. F **18**, 2303 (1988).
[51] Z.M. Stadnik and G. Stroink, Phys. Rev. B **38**, 10 447 (1988).
[52] Z.M. Stadnik, A.-P. Tsai, and A. Inoue, in *Proceedings of the International Conference on Aperiodic Crystals*, edited by G. Chapuis (World Scientific, Singapore, in press); Z. M. Stadnik, Hyperfine Interact. **90**, 215 (1994).
[53] A. Shastri, F. Borsa, D.R. Torgeson, J.E. Shield, and A.I. Goldman, Phys. Rev. B **50**, 15 651 (1994), and references therein.
[54] A. Shastri, F. Borsa, D.R. Torgeson, and A.I. Goldman, Phys. Rev. B **50**, 4224 (1994).
[55] N. Vernier, G. Bellessa, B. Perrin, A. Zarembovitch, and M. De Boissieu, Europhys. Lett. **22**, 187 (1993).
[56] S. Doniach and M. Šunjić, J. Phys. C **3**, 285 (1970).
[57] Y. Baer, G. Busch, and P. Cohn, Rev. Sci. Instrum. **46**, 466 (1975); S.A. Flodstrom, R.Z. Bachrach, R.S. Bauer, and S.B. Hagström, Phys. Rev. Lett. **37**, 1282 (1976); S.B.M. Hagström, R.Z. Bachrach, R.S. Bauer, and S.A. Flodström, Phys. Scr. **16**, 414 (1977).
[58] D.L. Ederer, R. Schaefer, K.-L. Tsang, C.H. Zhang, T.A. Caliicott, and E.T. Arakawa, Phys. Rev. B **37**, 8594 (1988).
[59] H. Matsubara, S. Ogawa, T. Kinoshita, K. Kishi, S. Takeuchi, K. Kimura, and S. Suga, Jpn. J. Appl. Phys. A **30**, L389 (1991).
[60] F.U. Hillebrecht, J.C. Fuggle, P.A. Bennett, Z. Zołnierek, and Ch. Freiburg, Phys. Rev. B **27**, 2179 (1983).
[61] Z.M. Stadnik and G. Stroink, J. Non-Cryst. Solids **99**, 233 (1988), and references therein.